Propulsion and Energy Forum
July 25-27, 2016, Salt Lake City, UT
52nd AIAA/SAE/ASEE Joint Propulsion Conference

Observation of Late-Time Ablation in Electric Solid Propellant Pulsed Microthrusters

Matthew S. Glascock,[1] Joshua L. Rovey,[2]
Missouri University of Science and Technology, Rolla, Missouri, 65409

Shae Williams[3] and Jason Thrasher,[4]
Digital Solid State Propulsion, Reno, Nevada, 89511

Electric solid propellants are an interesting potential option for propulsion because they are ignited by an applied electric current. The electric nature of these materials leads to the capability for use in pulsed electric propulsion devices. In this work, the ablation process of an electric solid propellant during pulsed microthruster operation is investigated using a triple Langmuir probe, thrust stand and high speed video camera. Results include quantitative time-of-flight, ablation mass per pulse and impulse-per-pulse measurements. Additionally, qualitative images from the high speed video are temporally correlated to these measurements. Analyses indicate 45±11% of the ablated mass per pulse is expelled at negligible speeds relative to the effective plume exhaust velocity (1500 m/s). Further, this occurs on a time scale that is three times longer than the 0.5 ms primary discharge. This late-time ablation has been identified in other pulsed microthrusters with traditional Teflon propellant, and the results presented here indicate that electric solid propellant exhibits similar behavior.

I. Introduction

Electric solid propellants (ESP's) are an emerging topic of research with major implications in the field of propulsion from the micro to macro scale[1,2]. These propellants offer new capabilities for controlling solid chemical rocket motors previously unheard of for typical energetic materials. When electric power at sufficient current and voltage levels is applied to an ESP, the solid propellant ignites and continues to exothermically decompose until that power is removed. This process can be repeated until the solid propellant is entirely consumed. Further, the burn rate of the propellant can be throttled by altering the electrical power applied. This method of operation is not possible with traditional solid rocket propellants and energetics, and greatly expands the potential applications for solid rocket motors that are fit with an ESP. Additionally, ESPs are insensitive to accidental ignition by spark, impact or even open flame. This is a huge advantage over most energetics in safety considerations and ease of use.

The development of ESPs began in the mid-late 90's with the investigation of a "green" automobile air bag inflator propellant (ABIP). This ammonium nitrate based material quickly garnered attention from the U.S. Air Force for other applications, including a patented[3] formulation for rocket propulsion application. Soon after, the first controlled extinguishable solid propellants were developed, the first of which was referred to as "ASPEN." This development process began adding ingredients to the ammonium nitrate based propellant to lower the melting point and increase the electrical conductivity during chemical combustion. Performance metrics of the ASPEN propellant were comparable to typical marks for solid rocket motors, but experienced major problems with initial ignition. Addressing these problems led to the development of a more advanced formula to achieve higher specific impulse and conductivity of the propellant. This higher performance electric propellant (HIPEP) is a hydroxyl ammonium nitrate (HAN) based energetic material. In this formulation, the ionic liquid oxidizer HAN exhibits a pyroelectric behavior; the application of electric power to this material incites the creation of nitric acid, triggering

[1] Graduate Research Assistant, Aerospace Plasma Laboratory, Mechanical and Aerospace Engineering, 160 Toomey Hall, 400 W. 13th Street, Student Member AIAA.
[2] Associate Professor of Aerospace Engineering, Mechanical and Aerospace Engineering, 292D Toomey Hall, 400 W. 13th Street, AIAA Associate Fellow.
[3] Chief Engineer, Aerospace Engineering, 5475 Louie Lane Suite D, Full Member AIAA.
[4] Engineer, Aerospace Engineering, 5475 Louie Lane Suite D, Full Member AIAA.

ignition of the formulation. This behavior has been previously observed in organic materials, but none of which are known to be energetic.

Electric solid propellants have also been tested for application in electric propulsion. All of the aforementioned ESP's have been tested as alternative fuel/propellant for the ablation fed pulsed plasma thruster and have shown performance marks comparable to that of the traditional propellant[2]. The Pulsed Plasma Thruster[4] (PPT) is a type of in-space electric propulsion system first flown in November of 1964 aboard the Soviet spacecraft Zond 2, marking the first application of electric propulsion on a spacecraft. Modern PPTs are primarily used for stationkeeping needs, attitude control, and other secondary propulsion system duties[5-7]. These thrusters have received considerable attention in the propulsion community due to the relative simplicity of the supporting technology and their ability to reliably generate small impulse bits.

Operation of the ablation-fed PPT begins with a high-current discharge between electrodes across the exposed surface of a solid propellant, usually Teflon® (PTFE). Typically, PPTs fall within two distinct classes of electric propulsion: electrothermal or electromagnetic[8]. The key difference lies in the acceleration mechanisms observed in PPT operation. LES 8/9 exhibits a typical behavior in that a portion of the plume is ionized by the main discharge (~10% in this case) and accelerated by the electromagnetic force arising from the $\boldsymbol{j} \times \boldsymbol{B}$ current front that propagates along with the ablated mass[8]. These high-energy, high-velocity particles contribute 15% (or more) of the kinetic energy of the exhaust gas despite the low mass relative to the rest of the plume, which remains neutral. On the other hand, the PPT-3/PPT-4 design is less common in that the acceleration of the ablated mass is dominated by electrothermal effects[9]. The temperature arising from the arc discharge is sufficiently high to provide enough energy to the particles to provide exhaust velocities comparable to or even exceeding that of chemical thrusters. These temperatures are typically limited by radiation and other dissipative processes to a few eV, but the high temperature neutrals provide nearly the entirety of the kinetic energy in the exhaust. Additionally, both thrusters (and most PPTs in general) have shown evidence of lost mass after the completion of the discharge pulse in the form of low relative velocity neutrals and even macroparticles[10]. This "late-time ablation" contributes little to nothing by way of performance. Further, this ablation is not readily measured, thus the mass fraction is not well characterized, but modeling efforts have estimated large fractions of the total ablated mass per pulse[11].

This paper focuses on the ablation of an electric solid propellant in PPT operation. Results from ablation mass, impulse-per-pulse and time-of-flight measurements are coupled with high speed imagery to show that the electric solid propellant exhibits late-time ablation. The experimental apparatus is described in Section II, and the Results and Analysis are given in Section III and IV, respectively. Conclusions from the work are described in Section V.

II. Experimental Apparatus

The PPT microthrusters are described, along with the ESP and power processing unit. Then the facilities in which the microthrusters are operated are described, followed by the diagnostics used to characterize the thrusters.

A. Microthrusters and Power Processing Unit

The microthrusters have a coaxial geometry as shown in Figure 1. The outer electrode is a 1/8" diameter aluminum tube and the concentric inner electrode is a 3/64" diameter molybdenum rod. The total length of the microthruster is about 1", with the propellant grain measuring roughly half of that length. The molybdenum inner electrode is also coated with polymer insulation (shellac) with a nominal thickness of 0.001". The ESP has a annular shape and fills the space between the inner and outer electrodes. By applying a relatively low voltage discharge from a capacitor bank (300 V) for a short duration pulse (about 0.5 ms) a small mass of the ESP is ablated and expelled from the thruster. In-house performance testing by the thruster manufacturer indicates that the impulse bit is around 500 μN-s per pulse, with a specific impulse on the order of 200 seconds. In general, the thrusters have an operation lifetime of between 250 and 300 pulses.

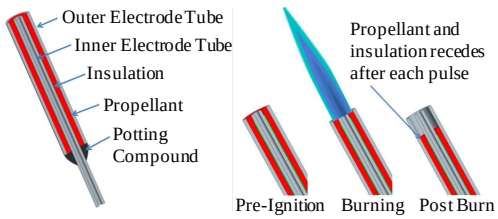

Figure 1: CAD Model illustrating composition and operation of the ESP microthruster.

The ESP is a hydroxyl ammonium nitrate (HAN)-based solution solid manufactured using benign processes and "green" ingredients, mixed in standard chemical glassware and cured conveniently at warm room temperatures (35°C/95°F). It has a chemical composition of HAN oxidizer (an inorganic ionic liquid) and polyvinyl alcohol (PVA) fuel binder, which make up 95% of the propellant, as shown in Table I. The ESP is initially a liquid and injected by syringe into the discharge gap of the microthruster. It is then cured to form a soft solid with the

appearance and texture of a soft pencil eraser. It is safe to handle and classified under DOT as a 1.4S explosive, making this ESP much more convenient to transport and work with than conventional solid rocket propellants.

Table I. Nominal composition of the High Performance Electric Propellant tested in the microthrusters.

Chemical Name	Chemical Formula	Percentage by mass	Molecular Mass, g/mol
Hydroxyl Ammonium Nitrate (HAN)	$(NH_3OH)^+ NO_3^-$	75%	96
Polyvinyl Alcohol (PVA)	$CH_2CH(OH)$	20%	44
Ammonium Nitrate (AN)	NH_4NO_3	5%	80

There are some key differences between the ESP and traditional Teflon® (PTFE) PPT propellant. PTFE is a fluorocarbon solid, while the ESP is a soft-solid mixture with composition given in Table I. In a typical PPT, the PTFE is an electrical insulator between the electrodes. The conductivity of the ESP in this work is comparable to "highly conductive" ionic liquids which have been selected as candidates for use in dye-sensitized solar cells[12]. With the ESP propellant the pulsed electric current can be conducted through the ESP, potentially initiating thermoelectric decomposition and creation of intermediates in the propellant. With PTFE an arc discharge is created near the surface of the solid PTFE, ablating the propellant via heat transfer. Additionally, in a conventional PPT, the propellant is fed into the thruster such that the arc discharge always occurs at the same physical location with respect to the thruster exit plane. With the ESP microthrusters the propellant face recedes from the exit plane over time as the propellant is burned away. It is currently unclear how these propellant differences affect the operation and performance of a PPT using the ESP as a propellant.

The power processing unit (PPU) used to operate the microthrusters is a custom in-house pulsed power supply. This PPU is primarily a bank of capacitors with a nominal rating of 900 μF. This bank is charged to 300 V with a small input power (5 V at < 1A). Once charged, the stored energy (about 40 J) is then rapidly discharged directly into the thruster electrodes, an event which typically lasts about 500 μs. This mode of operation was chosen as it was shown to increase the total impulse delivered over the thruster lifetime. Additionally, the voltage level of 300 V was chosen to keep the impulse bit per pulse around 500 μN-s. This PPU is vacuum-compatible and is mounted a few inches from the thruster during testing; the PPU is then remotely controlled via serial communication.

B. Vacuum Facilities

1. Missouri S&T Aerospace Plasma Lab

The microthrusters were tested in the large (1.8 m dia., 3 m lg.) space and high altitude vacuum facility at the Aerospace Plasma Laboratory of Missouri S&T. This facility uses four 89 cm diameter oil vapor diffusion pumps backed by an Edwards EH 4200 roots-blower pump and a Tokunda KP-7500BG rotary-vane pump. Standard operation for this work was two oil vapor diffusion pumps active which gives the facility a nominal base pressure of 2×10^{-5} Torr. The interior of the facility is equipped with a two-axis translation table system with a minimum step size of 2.6 μm that is controllable remotely to allow for the measurements made at varying locations.

2. Digital Solid State Propulsion (DSSP) Vacuum Facility

Microthrusters were also tested in the large vacuum facility at DSSP. This facility uses a single Varian VHS-250 oil vapor diffusion pump and an Alcatel ADS501 model rotary-vane, roots-blower pump combination for roughing of the chamber. Standard operation for this work was with the oil vapor diffusion pump active, yielding a nominal base pressure of 5×10^{-4} Torr. The interior of the facility is equipped with an optical table for mounting of hardware and diagnostics.

C. Diagnostics

Characterization of the plasma plume created during a pulse is generally the first step of analyzing a PPT system, and the primary focus of this work. Plume velocity distribution, plasma density and temperature, and current density are very useful in analyzing performance of a PPT. Work on plasma plume characterization of the microthruster has been conducted at Missouri S&T, who has partnered with DSSP to analyze the microthruster. A

number of prevalent PPT plume diagnostics were prepared and used for the analysis of the microthruster. In this work, a Langmuir triple probe was used to determine plasma densities and temperatures as well as for time of flight measurements. Additionally, a mass balance and high speed camera were used to investigate the ablated mass per pulse.

1. Langmuir Triple Probe

The Langmuir Triple Probe (LTP) is used to measure electron density and electron temperature at various locations in the plume as a function of time. The triple probe is well suited to operation in pulsed environments, and is a common diagnostic for the pulsed plasma thruster[13,14]. Tungsten wire of 0.5 mm diameter was inserted into three bores of a quad-bore alumina tube, creating the three isolated probe tips with 5.0 mm of exposed length. The remaining bore is plugged with a ceramic adhesive. On the other end of the probe, the tungsten wires connect to individual standard RF cables inside a grounded enclosure to ensure the connections are well shielded.

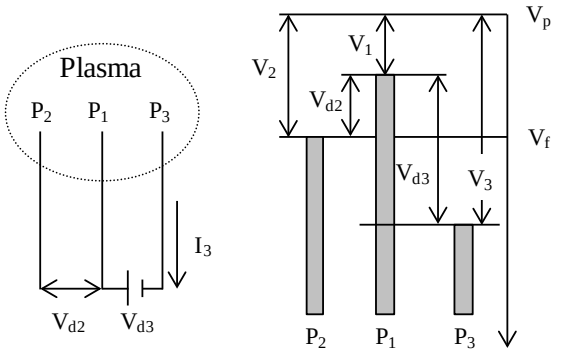

Figure 2: Electrical schematic and illustration of the triple Langmuir probe in voltage-mode.

In this work, the triple probe was operated in what is referred to as "voltage-mode," wherein (as in Figure 2) three identical probes are inserted into the plasma. All three probes are floating with respect to ground (V_f), and a bias voltage difference, V_{d3}, is applied externally to two of the probes via a battery. In this work, V_{d3} was selected as a nominal 27 V, supplied via three 9V batteries in series. During a pulse, the voltage difference V_{d2} is measured via a differential voltage probe and the probe current, I_3, is measured via a current monitor. The high voltage differential probe was selected because these probes were found to be less susceptible to signal noise than digitally subtracting signals on an oscilloscope, or using differential operational amplifiers. These measurements are displayed as a function of time during testing on a 4-channel Tektronix TDS2024B oscilloscope. Through the Langmuir Triple Probe theory from Chen and Sekiguchi[15] these measurements $V_{d2}(t)$ and $I_3(t)$ can be used to directly calculate the plasma electron temperature, $T_e(t)$, and the plasma density, $n_e(t)$. This process was conducted by the authors previously[16]. In the present work, the triple probe is used as a plume time-of-flight measurement device in order to evaluate the effective exhaust velocity of the microthruster. This is accomplished by examining the probe current, I_3. This signal is then temporally correlated to initiation of the thruster circuit discharge current, I_D, as measured by an IPC CM-1-MG current monitor to determine the plume time-of-flight.

2. Mass Balance

Additionally, the mass bit expelled per pulse is a quality of interest in the testing of the microthrusters. In order to estimate this, the mass of a microthruster is measured immediately prior to testing and again immediately following testing. The mass scale used was a Radwag AS310/C/2 which has a resolution of 0.1 mg and a quoted repeatability (standard deviation from 10 weighing cycles) of 0.1 mg. With careful tabulation of the number of pulses logged on a microthruster during testing, an estimate within 2% of the average mass expelled per pulse (the mass bit) value can be determined. This value will be important for the analysis of the thrust contribution of the plasma plume and analysis of the impulse-per-pulse.

3. Thrust Stand

The existing thrust stand previously built in-house for performance testing of the microthrusters was used in this work. This thrust stand is integrated into the DSSP vacuum facility, and was thus not available for testing in the S&T facility. The design is a pendulum using spring steel as a dampening method. The microthruster is mounted to a fixture suspended from an aluminum frame by two pieces of 2.5 cm wide spring steel to ensure minimal cross-axis movement. During each thruster discharge, the displacement of the fixture is measured by a laser displacement sensor with a resolution of 5 μm. This corresponds to a resolution in thrust measurement of about 1 mN for typical pendulum fixture mass. Estimated accuracy of the thrust stand is ±10% based on error analysis in the laser and chamber back pressure. In the current configuration, the thrust stand can measure the impulse-per-pulse (or impulse bit, I_{bit}) of the microthruster within a range of 0.025 mN-s to 5 mN-s.

4. High Speed Camera

The high speed camera for the visual ablation analysis of the microthruster is a Vision Research Inc. Phantom V7.3 model camera with a maximum framerate of 500,000 frames-per-second (fps). Due to restrictions on image resolution, however, the framerate used in this work was 125,000 fps. This correlates to an exposure time of 8 μs per image. The typical setting for the camera in this work was to capture 200 images during the thruster discharge (i.e. 1.6 ms of footage). Additionally, the camera was triggered digitally in sync with the microthruster via LabVIEW. Measurement of a digital output of the high-speed camera detailing when the camera is triggered allows for temporal correlation of the images to probe diagnostic data accurate to about one frame (±8 μs).

III. Results

In this section, experimental results from the mass balance, triple Langmuir probe and thrust stand are presented. These results include the average mass bit of all thrusters tested in recent time and some impulse-per-pulse results for a few of these that were measured. Experimental results are used to determine an effective exhaust velocity of the plume and temporally correlated to high speed images.

A. Ablation Mass

Table II details the results of the mass balance measurements made of twenty microthrusters tested, both during this work, as well as in previous work[16,17]. The average mass bit (m_{bit}) is calculated by subtracting the final from initial mass and dividing by the number of pulses. Overall, the average mass bit is 240.3 μg with a 95% confidence interval (CI) of ±76.8 μg. Note that some of the microthrusters shown here were tested in the DSSP facility, while the others were tested in the S&T facility. This result is on the order of typical values for a PTFE PPT, which is usually between 10 and 100 μg, though it is noticeably higher than typical values[4].

Table II: Average ablation mass bit data for twenty microthrusters.

Serial no.	Pulses	Initial Mass (mg)	Final Mass (mg)	Average Mass Bit (μg)
OD01A05	39	645	621	615.4
OD01A09	200	639	549	450.0
OD01A10	127	635	620	118.1
OD01A12	222	647	590	256.8
OD01A13	206	642	588	262.1
OD01A14	155	636	545	587.1
OD01A17	280	643	611	114.3
OD02A02	90	638	605	366.7
OD02A06	150	637	603	226.7
OD02A10	150	625	613	80.00
OD02A21	108	652	644	74.07
OD02A22	100	629	579	500.0
OD02A24	120	638	624	116.7
RR43A08	121	641	631	82.6
RR50A14	143	658	639	132.9
RR50A20	153	661	637	156.9
RR51A03	150	661	614	313.3
RR51A06	150	642	623	126.7
RR51A10	161	641	624	105.6
RR52A10	150	665	647	120.0
		95% Conf. Interval:		**240.3±76.8**

B. Langmuir Triple Probe

The Langmuir triple probe provides measurements of probe current (I_p) as a function of time for each pulse of a microthruster. Additionally, a current monitor measures the thruster circuit discharge current (I_D) for each pulse. Figure 3 shows typical traces of $I_p(t)$ and $I_D(t)$ measurements for a single pulse of thruster RR51A10. These data are used to calculate the time-of-flight of the thruster plume from the initiation of the discharge current (here, ~110 μs) and peak probe current (~150 μs).

Effective exhaust velocity (V_{ex}) was determined from these time-of-flight measurements, and the calculated data are shown in Figure 4. The three thrusters shown were tested in the DSSP facility such that the impulse bit could be measured simultaneously with time-of-flight. The triple probe signal was used to calculate the time-of-flight of the plume exhaust from the thruster exit to the probe. The distance of travel is known (5 cm), and we define the time-of-flight to be the time between when the discharge current measurement becomes positive (i.e. time zero) and the time of peak current measured by the triple probe (~20 to ~60 μs). Time-of-flight results indicate an average exhaust velocity over all pulses of about 1500 m/s. Inadequate temporal resolution of the data acquisition system limits the accuracy of the determination of time-of-flight to an ~10% uncertainty.

C. Impulse Bit

Thrust testing was conducted at DSSP. A primary focus of this thrust testing was to determine the impulse bit per pulse (I_{bit}) of the microthrusters. Figure 5 shows these results over the pulse lifetime of four different microthrusters from various batches. The first three (RR43A08, RR50A14 and RR51A10) were tested in the DSSP vacuum facility equipped with the triple Langmuir probe diagnostic. The final thruster (RR50A20) tested previously by DSSP, was not interrogated with the Langmuir probe. From the data shown in Figure 5, the impulse bit is between 0.15-0.27 mN-s with an average value of 0.21 and 95% CI of ± 0.01 mN-s. The trends seen here are commonly observed for these microthrusters[2].

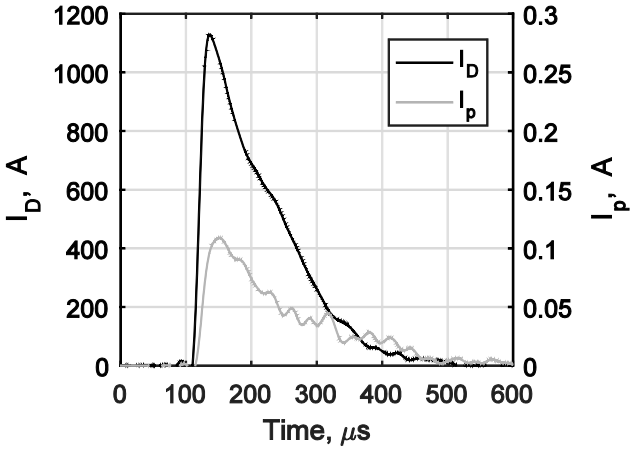

Figure 5: Typical thruster discharge and Langmuir triple probe current traces.

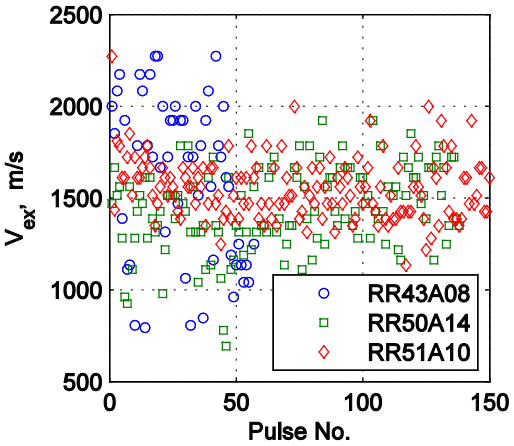

Figure 3: Effective exhaust velocity from Langmuir triple probe time-of-flight measurements.

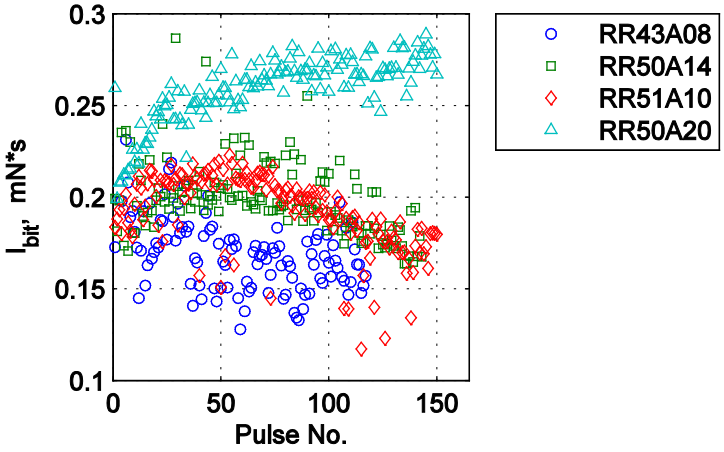

Figure 4: Measured impulse bit for four microthrusters.

D. High Speed Images

The Phantom high speed camera was used to capture images during the discharge of a small number of the thrusters tested. Using a combination of an NI DAQ system and Tektronix Oscilloscope, these images were correlated with the measured discharge current of the thruster circuit. Figure 6 shows nine images taken from a single discharge with timestamps and corresponding time marks on the discharge circuit measurement. Note that the beginning of the discharge occurs at roughly 0.117 ms, as indicated by the rapid rise in discharge current and verified by the appearance of a visible glow at the thruster exit. Additionally, both the discharge current and the high speed images indicate a peak (peak current, peak visible intensity) at 0.133 ms, seeming to validate the correlation between the visible glow and the measured discharge current.

More interesting, however, is that the glow of the discharge and the apparent expulsion of particles are visible long after the discharge ends. The measured discharge current becomes negligible at the 0.501 ms timestamp, with a bright glow still visible. Further, even long after the discharge current is no longer measured, visible particles are observed from the high speed imagery, continuing through to the final image taken, at a timestamp of 1.597 ms. The time-scale for the total ablation is roughly three or more times that of the primary discharge. The ablation observed post-discharge is a previously studied phenomenon in PTFE PPTs, and is generally referred to as "late-time" ablation. Qualitatively, from the high speed imagery, it would seem that this ablated mass is a significant fraction of the total ablated mass per pulse, though there is no way to directly measure this fraction from this diagnostic.

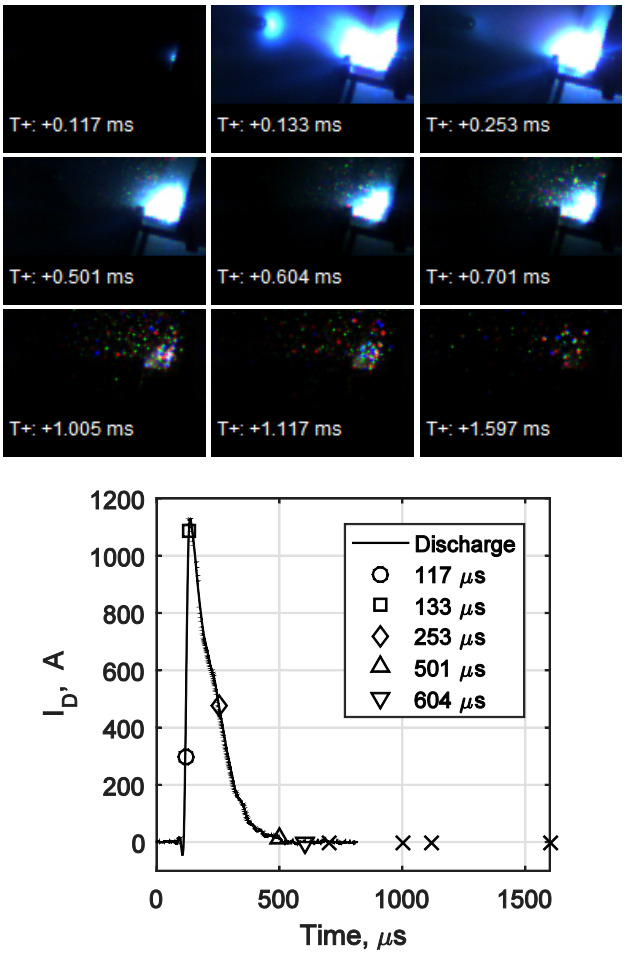

Figure 6: Selected images from high speed footage of a thruster pulse with temporally correlated data.

IV. Ablation Mass Analysis

The high speed imagery provides a qualitative indication of propellant ablation well after the main discharge has ended (late-time ablation). However, it is impossible to make a quantitative mass estimate for this ablated propellant without making restrictive and unfounded assumptions. Thus, it is desirable to apply thel above numerical results to obtain some estimate of this late-time ablation mass. Using the simple equation (1) below, from the definition of impulse, the *calculated* ablated mass per pulse can be determined from the *measured* impulse bit and exhaust velocity. This calculation will then be compared to the directly measured ablation mass from this and previous work.

$$m_{bit} = \frac{I_{bit}}{V_{ex}} \tag{1}$$

Recall that m_{bit} is the ablation mass per pulse, I_{bit} the impulse per pulse and V_{ex} the effective exhaust velocity. Using the average values measured for these quantities (0.21 mN-s, 1500 m/s), an average calculated mass bit of 140 µg is obtained. This calculated mass bit is 44-85% of the measured average ablation mass bit (240±76.8 µg). This

would indicate that the remaining 15-56% of the ablated propellant per pulse is ablating very slowly and not contributing to the measured impulse of each pulse. Looking at the specific cases of each microthruster, we find the average value to be 45±11% late-time ablation mass. Of course, this range is based on an average value, and some disagreement is to be expected for individual cases. For example, consider the three microthrusters for which both impulse-per-pulse and exhaust velocity measurement data are available: RR43A08, RR50A14 and RR51A10 (see Figure 4, Figure 5). From , we see the ablation mass measurements for these thrusters are 82.6, 132.9 and 105.6 μg, respectively. Comparing these values to the ablation mass calculated above indicates that all (or more) of the mass bit is necessary to produce the measured impulse bit at that velocity. This is nonsensical, and is likely due to a combination of measurement error and facility effects for these thrusters. More specifically, the DSSP test facility (where impulse bit can be measured) has a base pressure of more than twenty times that of the facility used to test the other microthrusters. This raised back pressure will reduce the effective exhaust velocity from time-of-flight measurements, falsely indicating that the entire ablation mass contributes to the measured impulse. Unfortunately, this data is only available for a select few thrusters. Nevertheless, we surmise that these are rough bounds for the actual late-time ablation mass fraction, and this sizeable fraction has been observed in PPTs previously.

The ablation process of PTFE has been investigated in detail by the PPT research community. Ablation modeling efforts have shown that the ablation is not an instantaneous process, but a gradual process correlated with the discharge current[11,18-20]. Experimental results have shown agreement with these conclusions[21]. Additionally, PPT experiments have identified residual heating, large particulate emission[10] and late-time material ablation[22] as causes of poor propellant efficiency in PPTs. Spanjers et. al[10] observed particulate emission in a PTFE PPT consuming 40±3% of the ablation mass and yet contributing less than 1% to thrust performance. Investigating postpulse temperature effects, Antonsen et. al[22] found that late-time ablation accounted for 23±11% of the lost propellant. Clearly, these effects have a considerable negative impact on efficiency in PPTs. We have observed that these processes still occur when using an electric solid propellant in a PPT, with similar mass fractions.

V. Conclusions

Plume diagnostics were performed on a novel electric solid propellant microthruster. Twenty microthrusters were tested in two separate facilities. A Langmuir triple probe was used to measure the time-of-flight of the plume and an impulse-per-pulse of 0.21 mN-s was measured using a thrust stand. The average mass bit was found to be 240 μg from mass balance measurements. Analysis of the time-of-flight data yields an effective velocity of 1500 m/s. Additionally, high speed imagery of a microthruster during discharge shows evidence of late-time ablation of the electric solid propellant in the form of bright particles being expelled from the device long after the main discharge dissipates.

Numerical analysis of the measured impulse bit and exhaust velocity yields a calculated ablation mass that contributes to the impulse of 140 μg. This number differs from the measured ablation mass substantially and indicates that much of the ablation mass is expelled at low velocities and does not contribute meaningfully to the performance. The mass fraction of this late-time ablation is estimated to be 45±11%. Traditional pulsed plasma thrusters using PTFE for propellant experience a similar phenomenon with mass fractions on this order. Thus, we conclude that electric solid propellant exhibits the same behavior on a similar magnitude. Particulate emission and late-time ablation have been identified as causes of poor propellant efficiency in PPTs. Reduction of this late-time ablation during pulsed plasma thruster operation is an avenue of performance improvement for electric solid propellant.

Acknowledgments

The authors would like to extend a very special thanks to Tim Manship of DSSP, who was essential in the proper operation of the Phantom high speed camera. Additionally, thanks to John Sousa of DSSP for the (numerous) repairs of the electronic equipment used in this work. Mr. Glascock would like to thank the NSTRF program, which partially supported this work through grant number NNX15AP31H.

References

[1]Sawka, W. N., Katzakian, A., and Grix, C., "Solid State Digital Cluster Thrusters for Small Satellites, Using High Performance Electrically Controlled Extinguishable Solid Propellants," *AIAA/USU Conference on Small Satellites*, AIAA, Logan, UT, 2005.

[2]Sawka, W. N., and McPherson, M., "Electrical Solid Propellants: A Safe, Micro to Macro Propulsion Technology," *49th AIAA/ASME/SAE/ASEE Joint Propulsion Conference*, AIAA, San Jose, CA, 2013. doi: 10.2514/6.2013-4168

[3]Sawka, W. N., U.S. Patent for a "Controllable Digital Solid State Cluster Thrusters for Rocket Propulsion and Gas Generation," No. 7958823 B2 and 8464640; June 14, 2011 and June 18, 2013.

[4]Burton, R. L., and Turchi, P. J., "Pulsed Plasma Thruster," *Journal of Propulsion and Power*, Vol. 14, No. 5, 1998, pp. 716-735. doi: 10.2514/2.5334

[5]Gatsonis, N. A., Lu, Y., Blandino, J., Demetriou, M. A., and Paschalidis, N., "Micropulsed Plasma Thrusters for Attitude Control of a Low-Earth-Orbiting Cubesat," *Journal of Spacecraft and Rockets*, Vol. 53, No. 1, 2016, pp. 57-73. doi: 10.2514/1.A33345

[6]Guman, W. J., and Nathanson, D. M., "Pulsed Plasma Microthruster Propulsion System for Synchronous Orbit Satellite," *Journal of Spacecraft and Rockets*, Vol. 7, No. 4, 1970, pp. 409-415. doi: 10.2514/3.29955

[7]LaRocca, A. V., "Pulsed Plasma Thruster System for Attitude and Station Control of Spacecraft," *First Western Space Congress*, 1970, pp. 688-702.

[8]Jahn, R. G., *Physics of Electric Propulsion*, New York: McGraw-Hill, 1968.

[9]Boyd, I. D., Keidar, M., and McKeon, W., "Modeling of a Pulsed Plasma Thruster from Plasma Generation to Plume Far Field," *35th Joint Propulsion Conference and Exhibit*, AIAA, 1999. doi: 10.2514/6.1999-2300

[10]Spanjers, G. G., Lotspeich, J. S., McFall, K. A., and Spores, R. A., "Propellant Losses Because of Particulate Emission in a Pulsed Plasma Thruster," *Journal of Propulsion and Power*, Vol. 14, No. 4, 1998, pp. 554-559. doi: 10.2514/2.5313

[11]Mikellides, P., and Turchi, P., "Modeling of Late-Time Ablation in Teflon Pulsed Plasma Thrusters," *32nd Joint Propulsion Conference and Exhibit*, AIAA, Lake Buena Vista, FL, 1996. doi: 10.2514/6.1996-2733

[12]Sigma-Aldrich, "Ionic Liquids for Electrochemical Applications," *Aldrich ChemFiles*, Vol. 5, No. 6, 2005.

[13]Eckman, R., Byrne, L., Gatsonis, N. A., and Pencil, E. J., "Triple Langmuir Probe Measurements in the Plume of a Pulsed Plasma Thruster," *Journal of Propulsion and Power*, Vol. 17, No. 4, 2001, pp. 762-771. doi: 10.2514/2.5831

[14]Gatsonis, N. A., Eckman, R., Yin, X., Pencil, E. J., and Myers, R. M., "Experimental Investigations and Numerical Modeling of Pulsed Plasma Thruster Plumes," *Journal of Spacecraft and Rockets*, Vol. 38, No. 3, 2001, pp. 454-464. doi: 10.2514/2.3704

[15]Chen, S.-L., and Sekiguchi, T., "Instantaneous Direct-Display System of Plasma Parameters by Means of Triple-Probe," *Journal of Applied Physics*, Vol. 36, No. 8, 1965, pp. 2363-2375. doi: 10.1063/1.1714492

[16]Glascock, M. S., Rovey, J. L., Williams, S., and Thrasher, J., "Plasma Plume Characterization of Electric Solid Propellant Micro Pulsed Plasma Thrusters," *51st AIAA/SAE/ASEE Joint Propulsion Conference*, AIAA, Orlando, FL, 2015. doi: 10.2514/6.2015-4185

[17]Glascock, M. S., Rovey, J. L., Williams, S., and Thrasher, J., "Characterization of Electric Solid Propellant Pulsed Microthrusters," *Journal of Propulsion and Power*, (to be published).

[18]Gatsonis, N. A., Juric, D., Stechmann, D., and Byrne, L., "Numerical Analysis of Teflon Ablation in Pulsed Plasma Thrusters," *43rd AIAA/ASME/SAE/ASEE Joint Propulsion Conference & Exhibit*, AIAA, Cincinnati, OH, 2007. doi: 10.2514/6.2007-5227

[19]Keidar, M., Boyd, I. D., and Beilis, I. I., "Electrical Discharge in the Teflon Cavity of a Coaxial Pulsed Plasma Thruster," *IEEE Transactions on Plasma Science*, Vol. 28, No. 2, 2000, pp. 376-385.

[20]Schönherr, T., Zach, W. A., Komurasaki, K., Hörner, S., Arakawa, Y., and Herdrich, G., "Mechanical Probe and Modeling Efforts for Evaluation of Plasma Creation and Acceleration in Ppt," *33rd International Electric Propulsion Conference*, Washington, D.C., 2013.

[21]Scharlemann, C. A., and York, T., "Mass Flux Measurements in the Plume of a Pulsed Plasma Thruster," *42nd AIAA/ASME/SAE/ASEE Joint Propulsion Conference & Exhibit*, AIAA, Sacramento, CA, 2006. doi: 10.2514/6.2006-4856

[22]Antonsen, E. L., Burton, R. L., Reed, G. A., and Spanjers, G. G., "Effects of Postpulse Surface Temperature on Micropulsed Plasma Thruster Operation," *Journal of Propulsion and Power*, Vol. 21, No. 5, 2005, pp. 877-883. doi: 10.2514/1.13032